ACS central science

Research Article

Cite This: ACS Cent. Sci. 2019, 5, 1407−1416

http://pubs.acs.org/journal/acscii

Synthetic, Zwitterionic Sp1 Oligosaccharides Adopt a Helical Structure Crucial for Antibody Interaction

Qingju Zhang,[†,∥] Ana Gimeno,[‡] Darielys Santana,[§] Zhen Wang,[†] Yury Valdés-Balbin,[§] Laura M. Rodríguez-Noda,[§] Thomas Hansen,[†] Li Kong,[†] Mengjie Shen,[†] Herman S. Overkleeft,[†] Vicente Vérez-Bencomo,[§] Gijsbert A. van der Marel,[†] Jesús Jiménez-Barbero,[‡,⊥,#] Fabrizio Chiodo,[†,∇] and Jeroen D. C. Codée*[,†]

[†]Leiden Institute of Chemistry, Leiden University, Einsteinweg 55, 2333 CC Leiden, The Netherlands

[‡]CIC bioGUNE, Bizkaia Technology Park, Building 801 A, 48170 Derio, Spain

[§]Finlay Vaccine Institute, 200 and 21 Street, Playa, Havana 11600, Cuba

[∥]The National Research Centre for Carbohydrate Synthesis, Jiangxi Normal University, No 99 Ziyang Avenue, Nanchang 330022, China

[⊥]Ikerbasque, Basque Foundation for Science, Maria Diaz de Haro 3, Bilbao, 48013 Bizkaia, Spain

[#]Department of Organic Chemistry II, Faculty of Science and Technology, University of the Basque Country, EHU−UPV, 48940 Leioa, Spain

[∇]Amsterdam Infection and Immunity Institute, Department of Molecular Cell Biology and Immunology, Amsterdam UMC, Location VUmc, 1007 MB Amsterdam, The Netherlands

Supporting Information

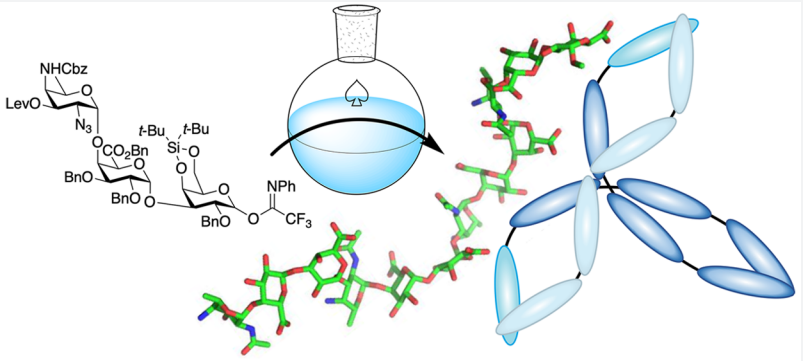

ABSTRACT: The zwitterionic *Streptococcus pneumoniae* serotype 1 polysaccharide (Sp1) is an important anchor point for our immune system to act against streptococcal infections. Antibodies can recognize Sp1 saccharides, and it has been postulated that Sp1 can elicit a T-cell-dependent immune reaction as it can be presented by MHC-II molecules. To unravel the molecular mode of action of this unique polysaccharide we here describe the chemical synthesis of a set of Sp1 fragments, ranging from 3 to 12 monosaccharides in length. We outline a unique synthetic approach to overcome the major synthetic challenges associated with the complex Sp1 structure and provide a stereoselective route of synthesis for the oligosaccharide backbone as well as a strategy to introduce the carboxylic acid functions. Molecular dynamics (MD) simulations together with NMR spectroscopy studies reveal that the oligosaccharides take up helical structures with the nona- and dodecasaccharide completing a full helical turn. The 3D structure of the oligosaccharides coincides with the topology required for good interaction with anti-Sp1 antibodies, which has been mapped in detail using STD-NMR. Our study has revealed the Sp1 nona- and dodecasaccharides as promising synthetic antigens, displaying all (3D) structural elements required to mimic the natural polysaccharide and required to unravel the molecular mode of action of these unique zwitterionic polysaccharides.

INTRODUCTION

Bacteria are surrounded by a thick layer of carbohydrates, which is important for their fitness, virulence, and pathogenicity.[1] Lipopolysaccharides, exopolysaccharides, and capsular polysaccharides (CPSs) protrude from the cell wall encapsulating the bacterium to provide a thick layer of defense. Forming the barrier between the bacteria and the extracellular milieu, carbohydrates shape the interactions with their environment, including the host immune system.[2] They

Received: May 7, 2019
Published: July 24, 2019

DOI: 10.1021/acscentsci.9b00454
ACS Cent. Sci. 2019, 5, 1407−1416

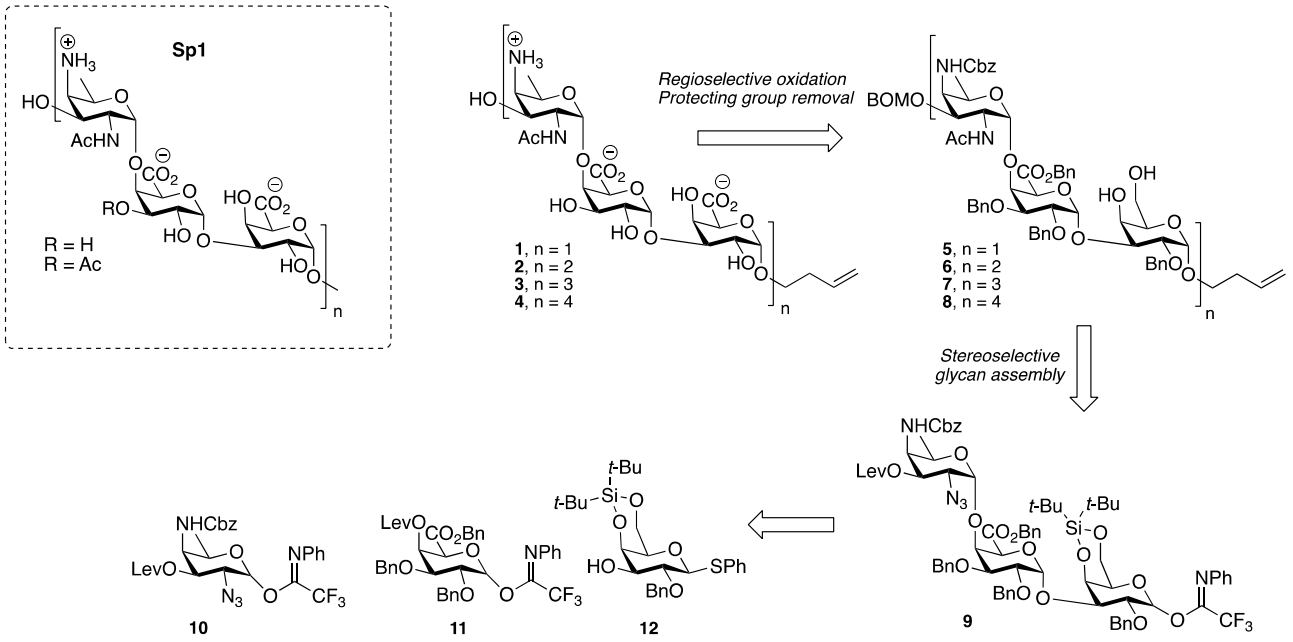

Figure 1. Structure of the Sp1 polysaccharide and the synthesis strategy to assemble structures **1**−**4**.

represent anchor points for carbohydrate binding receptors as well as anticarbohydrate antibodies. Because they are composed of unique repetitive structural motives, which are strain/serotype or species specific, and they are built up from monosaccharides that in most of the cases are not part of the mammalian carbohydrate repertoire, they form attractive antigens against which to direct vaccines. Generally, polysaccharides cannot be used as standalone vaccines, as they do not elicit a T-cell response, required for affinity maturation (class switching from IgM to IgG) and immunological memory, especially in infants, children, and the elderly population.[1,3] Therefore, polysaccharides are covalently conjugated to a carrier protein to recruit T-cell help and mount an effective immune response. Although bacterial polysaccharide vaccines are one of the biggest successes in modern medicine, the mode of action—or lack thereof—of conjugate vaccines remains relatively ill-understood. It is unclear how glycoconjugate vaccines are processed and which parts of the conjugate are presented by antigen presenting cells to T-cell receptors.[3] Also, the effect of carbohydrate loading on the efficacy of the conjugate vaccine is unclear, and optimizing vaccine activity largely remains a game of trial-and-error.[4−6] It is often impossible to predict what the optimal antigen is in a given polysaccharide, in terms of chain length (the number of repeating units), substitution pattern (e.g., degree of acetylation), and terminal residue (the one that is in principle most exposed on the glycoconjugate). The use of naturally sourced polysaccharide fragments in combination with random conjugation chemistry makes vaccine generation a relatively ill-defined process. Synthetic chemistry can be used to generate well-defined epitopes to establish immunological structure−activity relationships and deliver tailor-made optimal antigens, which can be conjugated in a site-selective manner, without altering the structure of the antigen.[4] Indeed, vaccines based on synthetic oligosaccharides are being developed and have been brought to the market.[7]

The WHO estimates that every year around 2 million deaths are caused by *Streptococcus pneumoniae*,[8] and every 2 min, three children die from pneumonia, making it the leading infectious cause of child mortality globally. Normally, it does not cause disease in healthy individuals, but in subjects with a weaker immune system (young children, elderly, and immunocompromised patients), it may cause deadly infections, such as pneumonia, septicemia, bacteremia, and meningitidis. *S. pneumoniae* serotype 1 (ST1) presents a unique polysaccharide (referred to as the Sp1 (poly)saccharide, see Figure 1), which is composed of the rare monosaccharide 2-acetamido-4-amino-2,4,6-trideoxy-D-galactose (D-AAT) and D-galacturonic acid residues.[9,10] Although Sp1 is a component in the currently licensed vaccines, Prevnar 13, Synflorix (conjugated), and Pneumovax 23 (nonconjugated), the exact active immunological epitope is unclear, and synthetic vaccines based on small fragments of Sp1 are under active investigation to improve the efficacy of anti-Sp1 glycoconjugate vaccines.[11] The unique Sp1 polysaccharide harbors both positively (the C-4-amino group of the D-AAT-residue) and negatively (on the galacturonic acids) charged groups, leading to zwitterionic motifs in the polysaccharide. The zwitterionic character of this polysaccharide provides this structure with exceptional immunological activity. In contrast to the vast majority of polysaccharides (*vide supra*), zwitterionic polysaccharides (ZPSs) are capable of inducing a T-cell-dependent immune response. They can be taken up by antigen presenting cells (APCs), processed, and presented in the context of major histocompatibility (MHC-II) proteins to T-cells, leading to T-cell activation.[12−16] It has been proposed that the three-dimensional structure of the Sp1 polysaccharide plays a decisive role in positioning the positively and negatively charged groups to interact with the presenting MHC-II molecule.[17] Likewise, the conformation of the polysaccharide may play an important role in shaping the structure of Sp1 epitopes for binding to antibodies. To unravel the molecular details behind the activation of both B-cells and T-cells by Sp1 saccharides, define optimal epitopes, and probe antibody and MHC-II binding, well-defined synthetic fragments are invaluable.[18] Although some syntheses have appeared over the years of the trisaccharide repeating unit, and a single route of synthesis has been disclosed for the assembly of a Sp1

DOI: 10.1021/acscentsci.9b00454
ACS Cent. Sci. 2019, 5, 1407−1416

Scheme 1. (A) Synthesis of Building Blocks 10, 11, and 12, and (B) Assembly of Oligosaccharides 1−4[a]

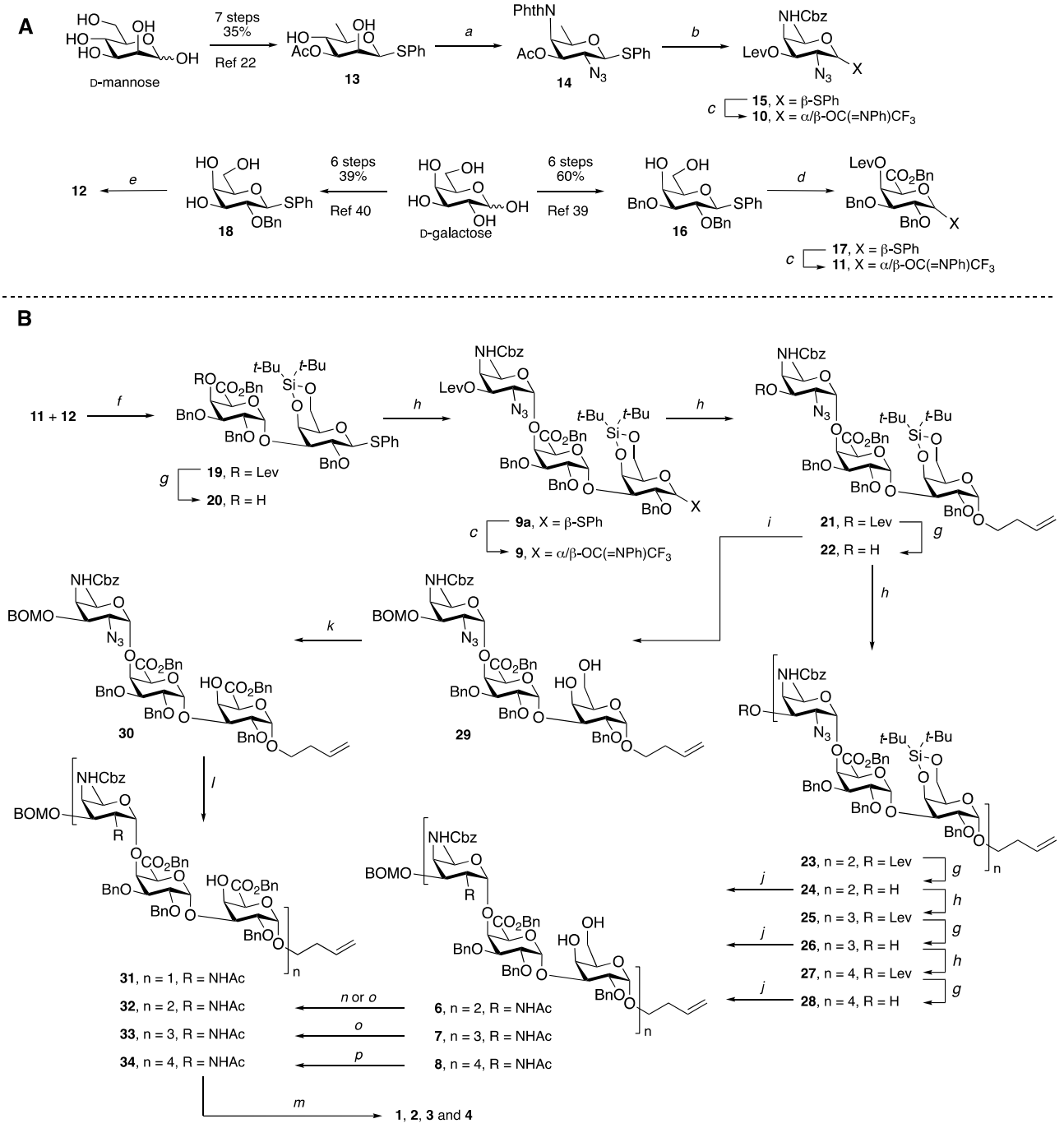

[a]Reagents and conditions: (a, i) Tf_2O, pyridine, DCM; (ii) $TBAN_3$, CH_3CN; (iii) PhthNK, DMF, 30% (over three steps). (b, i) Ethylenediamine, butanol, reflux; (ii) CbzCl, $NaHCO_3$, THF/H_2O, 69% (over two steps). (iii) LevOH, EDCI, DIPEA, DMAP, DCM, 91%. (c, i) NIS, TFA, DCM, 100%; (ii) *N*-phenyltrifluoroacetimidoyl chloride, K_2CO_3, acetone; **10**, 79%; **11**, 72%; **9**, 89%. (d, i) TEMPO, BAIB, DCM/*t*BuOH/H_2O, 4 °C; (ii) BnBr, Cs_2CO_3, DMF, 67% (over two steps); (iii) LevOH, EDCI, DIPEA, DMAP, DCM, 97%. (e) Di-*tert*-butylsilyl bis(trifluoromethanesulfonate), pyridine, 89%. (f) TfOH, DCM, −78 °C, 77% (α:β = 13:1). (g) $N_2H_4{\cdot}H_2O$, pyridine, AcOH, 0 °C to rt; **20**, 89%; **22**, 98%; **24**, 97%; **26**, 89%; **28**, 91%. (h) TBSOTf, DCM, 0 °C; **9a**, 85% (α:β = 13:1); **21**, 82%; **23**, 83%; **25**, 80%; **27**, 72%. (i, i) BOMCl, DIPEA, TBAI, DCM, 89%. (ii) HF/Py, pyridine, THF, 0 °C to rt, 94%. (j, i) BOMCl, DIPEA, TBAI, DCM; (ii) PPh_3, pyridine, H_2O, THF, reflux, 7 h; (iii) Ac_2O, pyridine; (iv) HF/Py, pyridine, THF, 0 °C to rt; **6**, 69%; **7**, 69%; **8**, 77%. (k, i) TEMPO, BAIB, DCM/*t*BuOH/H_2O, 4 °C; (ii) Cs_2CO_3, BnBr, DMF, 0 °C to rt, 84%. (l) AcSH, pyridine, 66%. (m, i) NaOH, THF, MeOH; (ii) Na, NH_3, THF, *t*BuOH, allylcarbinol or $CH_2{=}CHCH_2CH_2O{-}PEG_4{-}OCH_2CH_2CH{=}CH_2$; **1**, 95%; **2**, 39%; **3**, 55%; **4**, 47%. (n, i) TEMPO, BAIB, THF/*t*BuOH/DCE, 4 °C, then $NaClO_2$, *iso*-amylene, NaH_2PO_4, H_2O, 63%. (o, i) TEMPO, BAIB, $NaHCO_3$, EtOAc/*t*BuOH/H_2O, 4 °C; (iii) Cs_2CO_3, BnBr, DMF, 0 °C to rt; **32**, 45%; **33**, 51%. (p, i) TEMPO, BAIB, $NaHCO_3$, EtOAc/*t*BuOH/H_2O, 4 °C; (iii) $PhCHN_2$, DCM, Et_2O, 49%.

hexasaccharide, longer fragments encompassing multiple repeating units have so far proven out of synthetic reach, because of the tremendous synthetic challenge these molecules pose.[19−21]

DOI: 10.1021/acscentsci.9b00454
ACS Cent. Sci. 2019, 5, 1407−1416

We now report on the development of an effective synthesis route to assemble larger Sp1 oligosaccharides. The stereoselective strategy that we present has been used to generate Sp1 oligosaccharides ranging in length from a trisaccharide (one repeating unit) to a dodecasaccharide, encompassing four repeating units. The strategy allows for the incorporation of an alkene spacer at the "reducing" end of the saccharides, which can be used for future conjugation purposes. Through detailed structural studies, using molecular dynamics (MD) simulations in combination with NMR spectroscopy we show that the oligosaccharides take up a helical structure, with the ninemer (3 repeating units) completing a full turn. We next show that serum and antibody binding is length-dependent with the best epitopes presenting at least one helical turn. Our study has provided access to well-defined zwitterionic oligosaccharides capable of mimicking the three-dimensional structure of the natural polysaccharide. The availability of the fragments opens the way to further structural studies, including those directed at the presentation of the oligosaccharides by MHC-II molecules, and enables the generation of synthetic vaccines, presenting the structural epitopes as present in the natural polysaccharide.

RESULTS AND DISCUSSION

Synthesis. The structure of the Sp1 oligosaccharides represents a multitude of challenges, which have to be overcome in the development of an efficient route of synthesis, accessing sufficient amounts of the target oligosaccharides. First, the presence of rare D-AAT residues necessitates an effective route of synthesis for this building block.[22−24] Second the *cis*-glycosidic linkages demand an effective stereoselective glycosylation methodology.[25−27] Especially when the growing saccharide chains become larger, this represents a major synthetic hurdle. Third, an effective solution has to be found to introduce the carboxylic acid functionalities in the galacturonic acids residues. Galacturonic acid building blocks generally react poorly in glycosylation reactions, when used either as a donor or as an acceptor,[28,29] indicating that a postglycosylation−oxidation strategy, in which the glycan backbone is made before the introduction of the carboxylic acids, is most favorable. However, the late introduction of multiple carboxylic acids also represents a major challenge,[30] because every alcohol-to-acid conversion requires two oxidation events, and the polarity of the formed intermediates varies greatly. Finally, a suitable conjugation handle has to be introduced, which can be addressed chemoselectively in the presence of all other functionalities (amines, carboxylic acids, and hydroxyl groups).

The synthetic strategy we developed to access trisaccharide **1**, hexasaccharide **2**, nonasaccharide **3**, and dodecasaccharide **4** is depicted in Figure 1 and hinges on the use of the trisaccharide building block **9**. In our strategy we have combined a preglycosylation−oxidation approach to introduce one of the galacturonic acid residues in the repeating unit building block, with a postglycosylation−oxidation approach to introduce the second galacturonic acid moiety at the end of the glycan assembly.[31−33] This approach enables the use of a 4,6-silylidene-protected galactose donor moiety, which represents a highly reliable synthon for the stereoselective construction of 1,2-*cis*-galactosyl linkages[34−36] and increases the donor's reactivity. At the same time, it minimizes the amount of oxidative transformations that have to be executed at the end of the assembly, because half of the galacturonic acids have already been introduced at the building block level. We opted for the incorporation of a but-3-en-1-ol spacer because the double bond can be chemoselectively functionalized after glycan assembly, for example, using thiol−ene click chemistry.[37] The crucial trisaccharide building block **9** can be assembled using the three monomeric synthons **10**, **11**, and **12**.

Scheme 1 depicts the synthesis of the building blocks (Scheme 1A) and the assembly of the oligosaccharides (Scheme 1B). The AAT building block **10** was obtained from D-mannose following a slight adaptation of Kulkarni's protocol (see the SI for full synthetic details).[22] In 7 steps D-mannose was converted into diol **13**, which was transformed into the bis-triflate to set the stage for the introduction of the two masked amino groups. Regioselective substitution of the C-2-triflate using tetrabutyl ammonium azide ($TBAN_3$) and consecutive replacement of the C-4-triflate for an *N*-phthalimide functionality provided the AAT building block **14** in 30% yield.[38] Removal of the C-3-*O*-acetate and phthaloyl groups using ethylenediamine was followed by the introduction of the benzyloxycarbonyl group on the liberated C-4-amine and levulinoylation of the C-3-alcohol. Thioglycoside **15** was transformed into the corresponding *N*-phenyltrifluoroacetimidate **10** to allow for a chemoselective glycosylation toward the trisaccharide building block (*vide infra*). The assembly of the galacturonic acid building block **11** was achieved from known building block **16**,[39] available from D-galactose in 6 steps. Regioselective oxidation and formation of the benzyl ester was followed by levulinoylation of the free alcohol to provide the fully protected galacturonic acid **17**, which was transformed into imidate donor **11**. The silylidene-protected galactose thioglycoside **12** was obtained from 2-*O*-benzyl galactoside **18**,[40] generated from D-galactose in 6 steps. With the three monomeric building blocks in hand the synthesis of the pivotal trisaccharide building block was undertaken. First galacturonic acid **11** and silylidene galactose acceptor **12** were condensed to provide disaccharide **19**. Considerable optimization of the reaction conditions was required to install the desired glycosidic linkage with good stereoselectivity (see the SI for details), and ultimately dimer **19** was obtained in 77% yield (α:β = 13:1) on the multigram scale. Delevulinoylation then set the stage for the next chemoselective glycosylation event, in which the desired trisaccharide **9a** was obtained in 85% yield with good stereoselectivity (α:β = 13:1).[41] The thioglycoside **9a** was next transformed into imidate building block **9**. Assembly of the oligosaccharides started with the installation of the but-3-en-1-ol spacer. To this end donor **9** was condensed with allylcarbinol to give trisaccharide **21** in 82% as a single anomer, indicating the apt glycosylation properties of the donor building block. Delevulinoylation was followed by the next glycosylation event to give hexasaccharide **23** in 80% again as a single diastereoisomer.[42] A similar round of deprotection and glycosylation reactions then provided the nonasaccharide **25** (80%, α-only) and dodecasaccharide **27** (72%, α-only), showing the effectiveness of the silylidene donor and glycosylation strategy devised. To generate the target compounds **1**−**4** we then turned to the deprotection and functionalization chemistry. First, the free alcohol in trimer **22** was masked with a benzyloxymethyl ether, as it has previously been observed that deprotection of the C-3-OH of the AAT building block under basic conditions can lead to formation of the cyclic C3-*O*-C-4-*N*-carbamate.[20,21] Next the silylidene ketal was removed yielding diol **29**, of which the primary alcohol was regioselectively oxidized using the TEMPO/BAIB reagent combination to give, after formation of the benzyl ester to ease the purification, trisaccharide **30**. Global deprotection of this

DOI: 10.1021/acscentsci.9b00454
ACS Cent. Sci. 2019, 5, 1407−1416

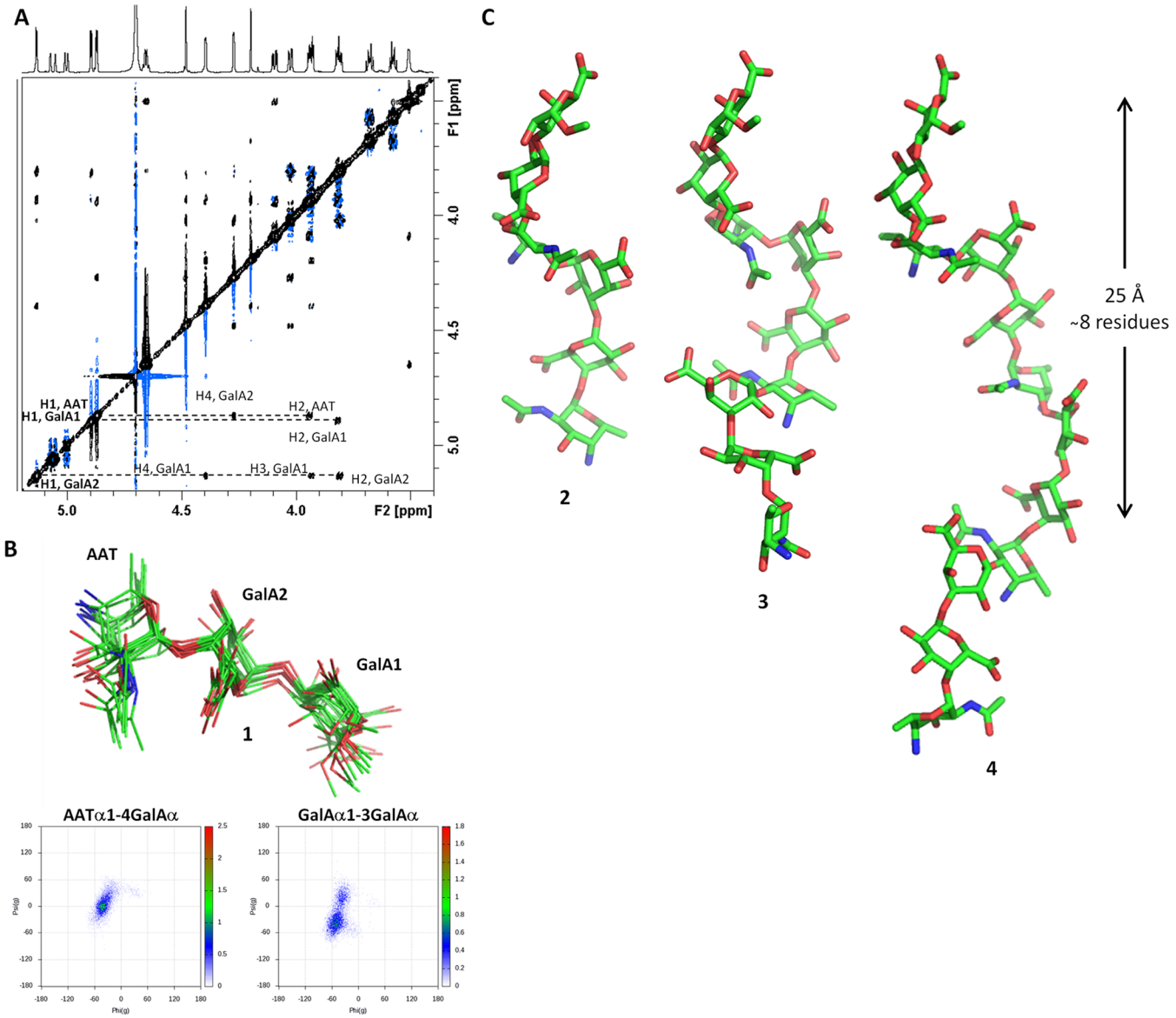

Figure 2. Structure of the zwitterionic oligosaccharides **1**–**4**. (A) NOESY spectrum of trimer **1** (500 ms mixing time) acquired at 800 MHz. Key inter-residue NOEs are indicated. (B) MD conformational analysis of **1** with the superimposition of 10 frames and plots of Φ/Ψ values explored along the 100 ns MD trajectory. The points are colored as a function of the population density. (C) Representative geometries of hexasaccharide **2**, nonasaccharide **3**, and dodecasaccharide **4** from the 500 ns MD simulations. The nonamer and dodecasaccharide make a full helical turn, comprising 8 monosaccharide residues and spanning ca. 25 Å. Both the major and minor *syn*(−)-Ψ and *syn*(+)-Ψ geometries for the GalAα1−3GalA moieties contribute to the helical geometry in the long oligosaccharides.

trimer was affected by transformation of the azide into the corresponding acetamide **31** using thioacetic acid,[43,44] after which the benzyl esters were saponified, and the remaining benzyl ethers, benzyloxycarbamate and benzyloxymethyl ether were removed using a dissolving metal reduction.[21,45] This last step proved challenging and required careful optimization. Addition of *tert*-butanol to the Birch reaction (using sodium in ammonia) was necessary to prevent removal of the acetyl from the AAT amino group, and addition of allylcarbinol as a "decoy substrate" diminished undesired reduction of the spacer double bond. Trisaccharide **1** was eventually obtained in 95% yield.

Next, the transformation of the larger oligosaccharides into target compounds **2**, **3**, and **4** was undertaken. First the levulinoyl group in the oligomers was replaced by a BOM ether as described above, and subsequently the azides were transformed into the acetamides. Whereas the use of thioacetic acid proved effective for the trisaccharide, it did not work well for the simultaneous reductions on the longer fragments. Therefore, we switched to a Staudinger reduction/acetylation sequence.[46,47] After desilylation, the oxidation precursors **6**, **7**, and **8** were obtained. Although the TEMPO/BAIB oxidation was effective in the synthesis of trisaccharide **1**, it failed in the assembly of the larger oligosaccharides, underscoring the difficulty in effecting multiple simultaneous oxidation reactions. We therefore explored the use of the two-step one-pot TEMPO/BAIB Pinnick oxidation protocol we recently introduced for reluctant substrates.[36] Following this two-step oxidation sequence, the hexamer **6** was successfully transformed into the dicarboxylic acid (63% yield), which was benzylated to give **32**. Unfortunately, the oxidation of the three alcohols in nonamer **7** could not be accomplished using the TEMPO/BAIB Pinnick reaction sequence, and a complex

DOI: 10.1021/acscentsci.9b00454
ACS Cent. Sci. 2019, 5, 1407−1416

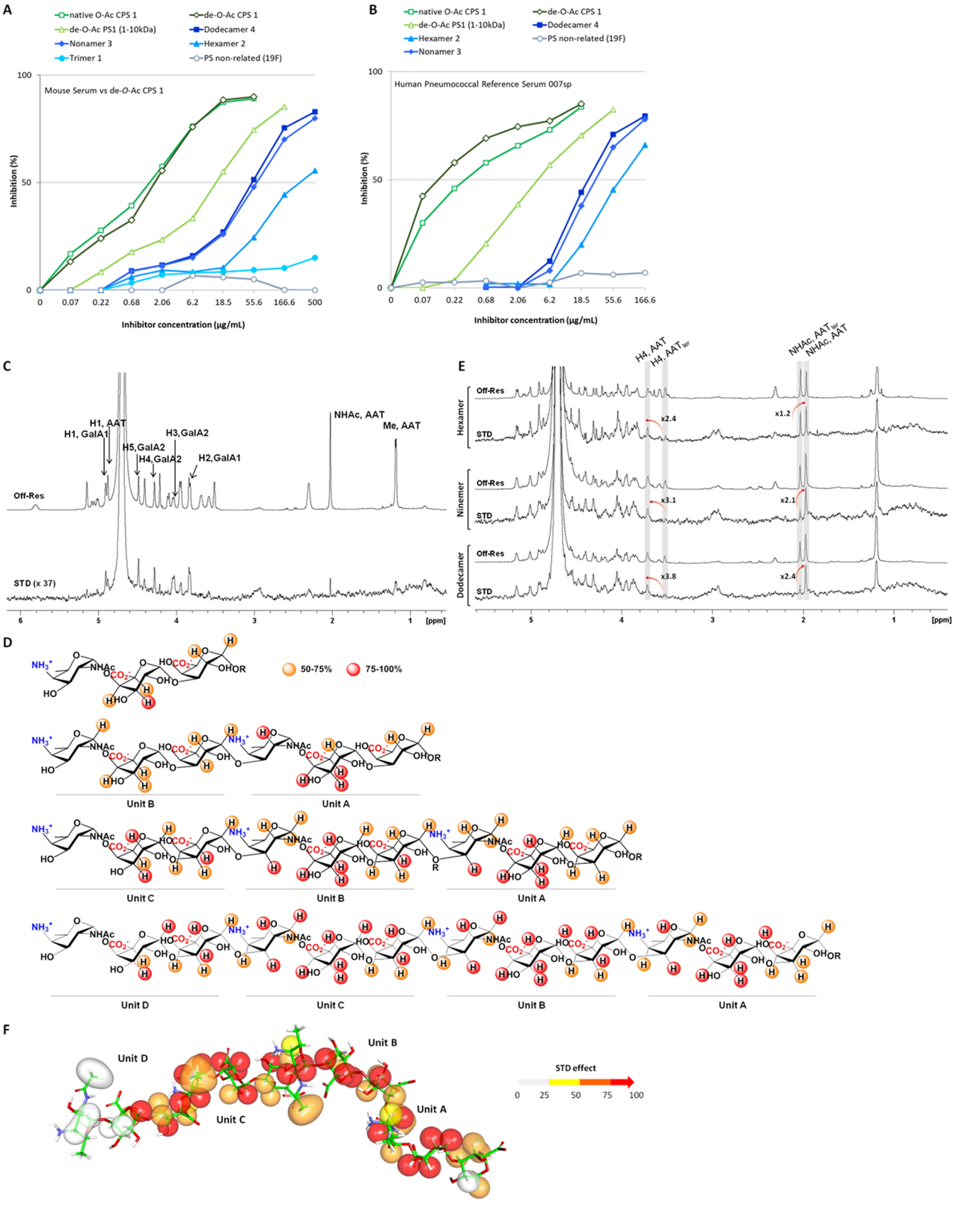

Figure 3. Binding studies of the synthetic oligosaccharides with the anti-Sp1 antibodies. (A) Competitive ELISA for antide-*O*-Ac Sp1 serum. (B) Competitive ELISA for the human pneumococcal reference serum 007sp. (C) STD and off-resonance NMR spectra for the interaction between anti-Sp1 IgG2a mAb and trimer **1**. (D) Structure of **1**−**4** where protons with the highest STD response are highlighted to delineate the binding epitope. The relative STD for overlapped protons was equally distributed in the structures of **3** and **4**. (E) STD and off-resonance NMR spectra for mixtures mAb:**2**, mAb:**3**, and mAb:**4**. The relative STD responses of H4 and NHAc protons of terminal and inner core AAT residues for hexamer **2**, nonamer **3**, and dodecamer **4** are highlighted. (F) Representative 3D structure of the dodecasaccharide **4**, in which the STDs are indicated by colors.

DOI: 10.1021/acscentsci.9b00454
ACS Cent. Sci. 2019, 5, 1407−1416

product mixture was obtained. It has previously been shown that efficiency of TEMPO mediated oxidations can be significantly improved under basic conditions. Presumably, the basic conditions[48] accelerate the formation of the hydrate from the intermediately formed aldehyde, enhancing the rate of the oxidation to the carboxylate. To test whether basic conditions could improve the challenging oxidations reactions required here, the hexasaccharide **6** was subjected to TEMPO/BAIB treatment in the presence of $NaHCO_3$. Under these conditions the dicarboxylic acid was obtained in a similar yield (67%) in comparison to the TEMPO/BAIB Pinnick sequence. Importantly nonasaccharide **7** could now be transformed into the tricarboxylic acid, and after benzylation, nonamer **33** was obtained in 51% yield (over two steps). Application of this protocol to the most complex substrate, dodecamer **8**, delivered, after benzylation using benzyl bromide and K_2CO_3, the octa-benzyl ester **34** in only 19% yield over the two steps. To further improve on the protocol, milder and more efficient benzylation conditions, using phenyldiazomethane,[49,50] were used. This way, dodecasaccharide **34** was obtained in 49% over the two steps. To complete the syntheses of hexamer **2**, nonamer **3**, and dodecamer **4**, the oligosaccharides were deprotected by saponification of the benzyl esters, and global reductive debenzylation provided the target oligomers in 39% (for **2**), 55% (for **3**), and 47% (for **4**) yield, respectively.

Structure. It has been proposed that the three-dimensional structure of the Sp1 polysaccharide is important for its T-cell activating activity.[17,51,52] Using NMR experiments combined with molecular dynamics (MD) calculations, it was proposed that the natural Sp1 polysaccharide takes up a right-handed helical structure with 8 monosaccharides per turn.[17] To probe whether the relatively short fragments **1**−**4** are capable of adopting a secondary structure we took a similar approach to establish the three-dimensional structure of the oligosaccharides. The NOESY spectrum of **1** showed key unequivocal inter-residue cross-peaks, which allowed defining the sugar conformation (Figure 2A). In particular, NOEs for H1AAT−H4GalA2, H1GalA2−H3GalA1, and H1GalA2−H4GalA1 proton pairs defined exo-*syn*-Φ/*syn*-Ψ conformations around both glycosidic linkages. Fittingly, the 100 ns MD simulation predicted exo-*syn*-Φ/*syn*-Ψ conformations for both linkages (Figure 2B). The Φ and Ψ dihedral angles for the AATα1−4GalA linkage remained fairly stable along the trajectory and mainly populated the exo-*syn*-Φ/*syn*(+)-Ψ conformation. In comparison, the GalAα1−3GalA linkage is slightly more flexible with transitions between *syn*(−)-Ψ and *syn*(+)-Ψ conformers occurring along the entire simulation. Although the conformational flexibility around Ψ is not fully discernible by NOESY experiments, NOE-estimated distances matched well with the average distances derived from the MD simulation of sugar **1** and pointed to the presence of *syn*(−)-Ψ and *syn*(+)-Ψ conformers (see Table S3). Thus, the MD simulation provided a proper model of the conformational features of **1**. Similarly, NMR analysis was combined with MD simulations to analyze the conformational features of the longer oligosaccharides **2**−**4**. It is noteworthy that ^{1}H and ^{13}C NMR signals of both central units (B and C) of dodecasaccharide **4** became indistinguishable. This is the case for the natural saccharide, where only one set of resonances is observed for the same residue of different units. NOESY experiments are fully compatible with the exo-*syn*-Φ/*syn*-Ψ conformations around AATα1−4GalA, GalAα1−3GalA, and GalAα1−3AAT glycosidic linkages in all the units, and the 500 ns MD simulation performed for **2**−**4** supported these results (see Tables S4−S6). As for **1**, the long oligosaccharides displayed exo*syn*-Φ/*syn*(+)-Ψ, exo-*syn*-Φ/*syn*(±)-Ψ, and exo-*syn*-Φ/*syn*(−)-Ψ conformations for the AATα1−4GalA, GalAα1−3GalA, and GalAα1−3AAT linkages, respectively. Thus, although the structural complexity increases by the addition of repeating units, the conformational flexibility around each glycosidic linkage remains essentially unaltered, with no correlation between remote residues. The analysis of the global structure of **3** and **4** revealed that they display a well-defined extended conformation (Figure 2C). Indeed, MD simulations predicted a large radius of gyration (RoG) and distances between both ends that extended beyond 30 and 40 Å, respectively (see Figure S3B). In particular, both sugars take up a right-handed helical structure with eight residues per turn, 5.04 Å of average separation between residues, and a pitch of ca. 25 Å (Figure 2), in line with the structure proposed for the Sp1 polysaccharide. Furthermore, and as also described for the natural polysaccharide, the positive and negative charges of the synthetic molecules are uniformly distributed, with the amino group of each AAT residue and the carboxyl groups of the previous and following GalA residues pointing at opposite sides of the helix (Figure S5).

Antibody Recognition. To probe binding of the synthetic oligosaccharides to antibodies directed at the capsular polysaccharide and establish how the length of the oligomers affects binding, inhibition ELISA experiments were performed. To generate serum against the de-*O*-acetylated natural polysaccharide (de-*O*-Ac Sp1) we conjugated the de-*O*-Ac Sp1 polysaccharide to tetanus toxoid, by periodate oxidation of the polysaccharide and a subsequent reductive amination conjugation step. Balb/c mice were immunized with the conjugate adsorbed on aluminum phosphate. Three immunizations were performed at 14 day intervals, and blood was collected 7 days postimmunization. ELISA wells were coated with the de-*O*-Ac Sp1 polysaccharide, and binding of the polyclonal antide-*O*-Ac-Sp1 serum was investigated in the presence of oligosaccharides **1**−**4**. Native and de-*O*-Ac Sp1 polysaccharides were used as positive controls, and the structurally nonrelated *S. pneumoniae* capsular polysaccharide 19F was employed as a negative control inhibitor. As depicted in Figure 3A, the shortest oligosaccharide **1** did not inhibit antibody binding to the surface bound polysaccharide, while the longer oligosaccharides were capable of binding the antibodies in the serum. A clear length dependence was observed for the longer oligosaccharides, with the longest fragments **3** and **4** showing best binding. Notably, there was relatively little difference between the nona- and dodecasaccharide **3** and **4**, and effective binding coincides with the length of the oligomers which can generate a full helical turn. Next, we probed the human pneumococcal serum 007sp,[53] raised against the 23-valent *S. pneumoniae* vaccine Pneumovax II, for binding to oligosaccharides **2**−**4** (Figure 3B). To this end ELISA wells were coated with the native Sp1 polysaccharide, and binding of serum antibodies was investigated in the presence of oligosaccharide inhibitors. As shown in Figure 3B, also here a specific length-dependent inhibition was observed with the fragments completing the full helical turn, binding significantly better than the shorter fragment.

To explore binding of the synthetic compounds in more detail, the interaction of the synthetic Sp1 oligomers **1**−**4** with

DOI: 10.1021/acscentsci.9b00454
ACS Cent. Sci. 2019, 5, 1407−1416

an anti-Sp1 IgG2a monoclonal antibody[54] was evaluated by STD-NMR experiments.[55] First, we analyzed the binding with the smallest glycan, trimer **1**. STD experiments for the 1:200 mixture of mAb:**1** provided very clear STD signals for H3−H5 of GalA2 and H1−H2 of GalA1 residues. These results suggest that both GalA are involved in the binding, with H3−H5 and H1−H2 of GalA2 and GalA1, respectively, pointing toward the protein surface, whereas the AAT moiety seems to be solvent exposed (see Figure 3C,D). In addition, trNOESY experiments for a 1:200 mixture of anti-Sp1 mAb:trimer **1** were applied to identify, if any, changes on the conformation of the sugar in the free and bound states. The inspection of NOE cross-peaks indicated that the bound conformation is very similar to the most populated conformation in solution. In particular, NOEs for H1AAT−H4GalA2, H1GalA2−H3GalA1, and H1GalA2−H4GalA1 proton pairs observed for the free sugar at 800 MHz and defining the exo-*syn*-Φ/*syn*-Ψ conformation around both glycosidic linkages are also present in the bound conformation (see Figure S10).[56] Next, the interaction of hexamer **2** with the anti-Sp1 mAb was analyzed (see Figure 3D and Figure S12). As for trimer **1**, H3−H5 protons of the GalA2 of unit A showed the strongest STD effect, and important signals were also observed for H1−H2 protons of GalA1 (unit A). Thus, both **1** and **2** bind comparably to the antibody, where the GalA2 moiety seems essential for the recognition. In addition, the H3−H5 protons of GalA2 and H1−H2, H5 of GalA1 of unit B showed significant STD responses, indicating that these residues are also involved in the binding event. In contrast, the STD effect of AAT residues was lower, especially that of unit B at the "nonreducing" end, indicating that this residue is more solvent exposed. These results indicate that both repeating units A and B in **2** take part in the interaction with the antibody and suggest an extended binding epitope for hexamer **2**. Notably, most of the protons with the highest STD intensities are located at the same molecule face that would be oriented toward the antibody (see Figure S12). Analogous STD experiments were performed for compounds **3** and **4** and provided clear evidence of the interaction. However, because of the high level of peak overlapping in the ^{1}H-STD spectra, detailed analysis of the binding epitope was hampered (see Figures S13 and S14). Overall, the STD epitope determined for nonamer **3** resembles that depicted above for hexamer **2** (Figure 3D). Several nonoverlapped protons of residues of units A, B, and C showed significant STD responses, strongly suggesting the presence of an extended binding epitope. It is noteworthy that the most intense STD signals were found for protons of the GalA2 residues, especially for those of the inner units A and B. In line with the binding of the trisaccharide **1** and hexasaccharide **2**, the protons of the AAT residue at the terminal end of the sugar (unit C) received the lowest saturation, indicating that this residue is again more exposed to the solvent. Finally, the STD experiments for a 1:30 mixture of mAb:**4** indicated that dodecamer **4** binds in a similar fashion to the antibody. Protons of the AAT moiety at the terminal end (unit D) showed the lowest saturation, whereas important STD was detected for protons belonging to several residues of units A−D, indicating an extended epitope (Figure 3D). It is noteworthy that when STD effects for compounds **2**−**4** are compared, insight is gained on the length of the antigen binding epitope. The STD response of protons of the terminal AAT and those of inner AAT residues differed, as a function of the length of the saccharides, showing a different involvement of the terminal AAT in the binding of each ligand (see Figure 3E). The STD responses of H4 and NHAc protons of the terminal and inner core AAT residues are fairly similar for hexamer **2**. This indicates that both residues are equally close to the protein surface. In contrast, the STD response of these residues became considerably different for nonamer **3**, where the terminal AAT, with a lower STD effect, is more exposed to the solvent. Similarly, dodecamer **4** showed different responses for the terminal and internal AAT residues. Together, these data indicated that the antigen binding site of the antibody is able to accommodate two repeating units as in compound **2**, but not entirely the third one as in compound **3**, where the terminal AAT residue is further away from the protein surface. These results thus point to a minimal binding epitope of 7−8 residues length, coinciding with the number of residues per turn of the helix displayed by the longer and native Sp1 oligosaccharides. Therefore, all results suggest a groovelike antigen binding site topology[57] for the antibody capable of binding a fragment of polysaccharide encompassing a full helical turn.[58−60]

CONCLUSION

This study has delivered a strategy for the assembly of large synthetic zwitterionic Sp1 oligosaccharides. The combination of a preglycosylation−oxidation strategy to introduce one of the carboxylate groups in the repeating unit with a postglycosylation−oxidation strategy to enable the fully stereoselective union of the trimer repeats has proven effective to assemble these complex oligosaccharides. Novel conditions have been employed to simultaneously introduce multiple carboxylates in a complex oligosaccharide through a modified TEMPO/BAIB oxidation. The devised conditions for this transformation can find further application in the assembly of complex oligosaccharide targets, such as heparins and other anionic bacterial capsular polysaccharides. Detailed structural studies revealed the synthetic Sp1 fragments to take up helical structures with the ninemer completing a full turn. The Sp1 oligosaccharide helices closely match the structures of the Sp1 polysaccharide placing the positively charged amino groups and negatively charged carboxylates of a repeating unit on different sides of the helix (see Figure 2C and Figure S5). It is shown that the binding of the oligosaccharides to both human and murine antibodies is length-dependent with the best binders being those oligosaccharides that can structurally complete a full helical turn, i.e., ninemer **3** and dodecasaccharide **4**. STD-NMR studies have confirmed the size of the best "minimal epitope" to encompass 7−8 monosaccharide residues and suggest a groove-type recognition mode where almost three repeating units of the oligo- or polysaccharides can be accommodated in the antibody binding site. It was recently reported that a structure as small as a single repeating unit may be used in a synthetic conjugate vaccine targeting *S. pneumoniae* serotype 1.[11] Although this conjugate could be used to raise opsonophagocytic anti-Sp1 antibodies in rabbits, the use of larger Sp1 fragments may trigger higher IgG titers having a better avidity for the Sp1 capsule. Higher IgG titers and more avid IgG are a key concept to remove nasopharyngeal carriage and decrease the transmission of *S. pneumoniae*. Our study reveals nonasaccharide **3** to be a very attractive candidate for the generation of an anti-Sp1 vaccine modality, and to this end the alkene conjugation handle may be exploited to hook up the saccharide to a carrier protein. The availability of the helical oligosaccharides will also enable structural studies to unravel the binding of these saccharides to

DOI: 10.1021/acscentsci.9b00454
ACS Cent. Sci. 2019, 5, 1407−1416

MHC-II molecules. It has been proposed that zwitterionic polysaccharides and teichoic acids can bind to these molecules allowing their presentation to T-cell receptors, triggering a T-cell response. The well-defined structures disclosed here will be instrumental in unravelling the enigmatic immunological behavior of these unique polysaccharides.

■ ASSOCIATED CONTENT

Supporting Information

The Supporting Information is available free of charge on the ACS Publications website at DOI: 10.1021/acscentsci.9b00454.

Experimental procedures and characterization for all new compounds, detailed description of NMR- experiments, molecular modeling studies and generation of serum against de-*O*-acetylated Sp1, description of antibody−oligosaccharide interaction studies, and copies of NMR spectra (^{1}H, ^{13}C, COSY, HSQC) of all new compounds (PDF)

■ AUTHOR INFORMATION

Corresponding Author

*E-mail: jcodee@chem.leidenuniv.nl.

ORCID

Thomas Hansen: 0000-0002-6291-1569
Herman S. Overkleeft: 0000-0001-6976-7005
Jesús Jiménez-Barbero: 0000-0001-5421-8513
Jeroen D. C. Codée: 0000-0003-3531-2138

Notes

The authors declare no competing financial interest.

■ ACKNOWLEDGMENTS

This work was financially supported by The European Research Council (ERC AdG "CHEMBIOSPHING", to H.S.O.), the Agencia Estatal de Investigacion (Grants CTQ2015-64597-C2-1P and RTI2018-094751-B-C21 to J.J.-B.), and ISCIII of Spain and the European Research Council (RECGLYCANMR, ERC ADG 788143 to J.J.B-.) and NWO−CW (Veni Grant 722.014.008 to F.C.).

■ REFERENCES

(1) Goldblatt, D. Bacteria polysaccharides, vaccines and boosting: measuring and maintaining population immunity. *Arch. Dis. Child.* **2008**, *93*, 646−647.

(2) Messner, P.; Schäffer, C.; Kosma, P. Bacterial cell-envelope glycoconjugates. *Adv. Carbohydr. Chem. Biochem.* **2013**, *69*, 209−272.

(3) Rappuoli, R. Glycoconjugate vaccines: Principles and mechanisms. *Sci. Transl. Med.* **2018**, *10*, No. eaat4615.

(4) Adamo, R. Advancing homogeneous antimicrobial glycoconjugate vaccines. *Acc. Chem. Res.* **2017**, *50*, 1270−1279.

(5) Costantino, P.; Rappuoli, R.; Berti, F. The design of semi-synthetic and synthetic glycoconjugate vaccines. *Expert Opin. Drug Discovery* **2011**, *6*, 1045−1066.

(6) Anish, C.; Schumann, B.; Pereira, C. L.; Seeberger, P. H. Chemical biology approaches to designing defined carbohydrate vaccines. *Chem. Biol.* **2014**, *21*, 38−50.

(7) Verez-Bencomo, V.; Fernández-Santana, V.; Hardy, E.; Toledo, M. E.; Rodríguez, M. C.; Heyngnez, L.; Rodriguez, A.; Baly, A.; Herrera, L.; Izquierdo, M.; Villar, A.; Valdés, Y.; Cosme, K.; Deler, M. L.; Montane, M.; Garcia, E.; Ramos, A.; Aguilar, A.; Medina, E.; Toraño, G.; Sosa, I.; Hernandez, I.; Martínez, R.; Muzachio, A.; Carmenates, A.; Costa, L.; Cardoso, F.; Campa, C.; Diaz, M.; Roy, R. A synthetic conjugate polysaccharide vaccine against Haemophilus influenzae type b. *Science* **2004**, *305*, 522−525.

(8) GBD 2015 LRI Collaborators. Estimates of the global, regional, and national morbidity, mortality, and aetiologies of lower respiratory tract infections in 195 countries: a systematic analysis for the Global Burden of Disease Study 2015. *Lancet Infect. Dis.* **2017**, *17*, 1133−1161.

(9) Geno, K. A.; Gilbert, G. L.; Song, J. Y.; Skovsted, I. C.; Klugman, K. P.; Jones, C.; Konradsen, H. B.; Nahm, M. H. Pneumococcal capsules and their types: past, present, and future. *Clin. Microbiol. Rev.* **2015**, *28*, 871−99.

(10) Stroop, C. J. M.; Xu, Q.; Retzlaff, M.; Abeygunawardana, C.; Bush, C. A. Structural analysis and chemical depolymerization of the capsular polysaccharide of Streptococcus pneumoniae type 1. *Carbohydr. Res.* **2002**, *337*, 335−344.

(11) Schumann, B.; Reppe, K.; Kaplonek, P.; Wahlbrink, A.; Anish, C.; Witzenrath, M.; Pereira, C. L.; Seeberger, P. H. Development of an efficacious, semisynthetic glycoconjugate vaccine candidate against Streptococcus pneumoniae Serotype 1. *ACS Cent. Sci.* **2018**, *4*, 357−361.

(12) Tzianabos, A.; Onderdonk, A.; Rosner, B.; Cisneros, R.; Kasper, D. L. Structural features of polysaccharides that induce intra-abdominal abscesses. *Science* **1993**, *262*, 416−419.

(13) Cobb, B. A.; Wang, Q.; Tzianabos, A. O.; Kasper, D. L. Polysaccharide processing and presentation by the MHCII Pathway. *Cell* **2004**, *117*, 677−687.

(14) Kreisman, L. S.; Friedman, J. H.; Neaga, A.; Cobb, B. A. Characteristics of carbohydrate antigen binding to the presentation protein HLA-DR. *Glycobiology* **2007**, *17*, 46−55.

(15) Tzianabos, A.; Wang, J. Y.; Kasper, D. L. Biological chemistry of immunomodulation by zwitterionic polysaccharides. *Carbohydr. Res.* **2003**, *338*, 2531−2538.

(16) Cobb, B. A.; Kasper, D. L. Zwitterionic capsular polysaccharides: the new MHCII-dependent antigens. *Cell. Microbiol.* **2005**, *7*, 1398−1403.

(17) Choi, Y. H.; Roehrl, M. H.; Kasper, D. L.; Wang, J. Y. A unique structural pattern shared by T-cell-activating and abscess-regulating zwitterionic polysaccharides. *Biochemistry* **2002**, *41*, 15144−15151.

(18) Zhang, Q.; Overkleeft, H. S.; van der Marel, G. A.; Codée, J. D. C. Synthetic zwitterionic polysaccharides. *Curr. Opin. Chem. Biol.* **2017**, *40*, 95−101.

(19) Wu, X.; Cui, L.; Lipinski, T.; Bundle, D. R. Synthesis of monomeric and dimeric repeating units of the zwitterionic type 1 capsular polysaccharide from Streptococcus pneumoniae. *Chem. - Eur. J.* **2010**, *16*, 3476−3488.

(20) Christina, A. E.; van den Bos, L. J.; Overkleeft, H. S.; van der Marel, G. A.; Codée, J. D. C. Galacturonic acid lactones in the synthesis of all trisaccharide repeating Units of the zwitterionic polysaccharide Sp1. *J. Org. Chem.* **2011**, *76*, 1692−1706.

(21) Schumann, B.; Pragani, R.; Anish, C.; Pereira, C. L.; Seeberger, P. H. Synthesis of conjugation-ready zwitterionic oligosaccharides by chemoselective thioglycoside activation. *Chem. Sci.* **2014**, *5*, 1992−2002.

(22) Emmadi, M.; Kulkarni, S. S. Synthesis of orthogonally protected bacterial, rare-sugar and D-glycosamine building blocks. *Nat. Protoc.* **2013**, *8*, 1870−1889.

(23) Emmadi, M.; Kulkarni, S. S. Recent advances in synthesis of bacterial rare sugar building blocks and their applications. *Nat. Prod. Rep.* **2014**, *31*, 870−879.

(24) Christina, A. E.; Blas Ferrando, V. M.; de Bordes, F.; Spruit, W. A.; Overkleeft, H. S.; van der Marel, G. A.; Codée, J. D. C. Multi-gram scale synthesis of an orthogonally protected 2-acetamido-4-amino-2,4,6-trideoxy-D-galactose (AAT) building block. *Carbohydr. Res.* **2012**, *356*, 282−287.

(25) Demchencko, A. V., Ed. *Handbook of chemical glycosylation: Advances in stereoselectivity and therapeutic relevance*; Wiley-VCH, 2008.

(26) Bennet, C. S., Ed. *Selective glycosylations: Synthetic methods and catalysts*; Wiley-VCH, 2017.

DOI: 10.1021/acscentsci.9b00454
ACS Cent. Sci. 2019, 5, 1407−1416

(27) Nigudkar, S. S.; Demchenko, A. V. Stereocontrolled 1,2-cis-glycosylation as the driving force of progress in synthetic carbohydrate chemistry. *Chem. Sci.* **2015**, *6*, 2687−2704.
(28) Van der Vorm, S.; Van Hengst, J. M. A.; Bakker, M.; Overkleeft, H. S.; van der Marel, G. A.; Codée, J. D. C. Mapping the relationship between glycosyl acceptor reactivity andglycosylation stereoselectivity. *Angew. Chem., Int. Ed.* **2018**, *57*, 8240−8244.
(29) Magaud, D.; Dolmazon, R.; Anker, D.; Doutheau, A.; Dory, Y. L.; Deslongchamps, P. Differential reactivity of α- and β-anomers of glycosyl acceptors in glycosylations. A remote consequence of the *endo*-anomeric effect? *Org. Lett.* **2000**, *2*, 2275−2277.
(30) Huang, L.; Teumelsan, N.; Huang, X. A facile method for oxidation of primary alcohols to carboxylic acids and its application in glycosaminoglycan syntheses. *Chem. - Eur. J.* **2006**, *12*, 5246−5252.
(31) Codée, J. D. C.; Christina, A. E.; Walvoort, M. T. C.; Overkleeft, H. S.; van der Marel, G. A. Uronic acids in oligosaccharide and glycoconjugate synthesis. In *Reactivity tuning in oligosaccharide assembly. Topics in Current Chemistry*; Fraser-Reid, B., Cristóbal López, J., Eds.; Springer: Berlin, Heidelberg, 2010; Vol. *301*.
(32) van den Bos, L. J.; Codée, J. D. C.; Litjens, R. E. J. N.; Dinkelaar, J.; Overkleeft, H. S.; van der Marel, G. A. Uronic acids in oligosaccharide synthesis. *Eur. J. Org. Chem.* **2007**, *2007*, 3963−3976.
(33) Nowogrodzki, M.; Mlynarski, J. Synthesis and application of uronic acids. *Curr. Org. Chem.* **2014**, *18*, 1913−1934.
(34) Imamura, A.; Ando, H.; Korogi, S.; Tanabe, G.; Muraoka, O.; Ishida, H.; Kiso, M. Di-*tert*-butylsilylene (DTBS) group-directed α-selective galactosylation unaffected by C-2 participating functionalities. *Tetrahedron Lett.* **2003**, *44*, 6725−6728.
(35) Imamura, A.; Matsuzawa, N.; Sakai, S.; Udagawa, T.; Nakashima, S.; Ando, H.; Ishida, H.; Kiso, M. The origin of high stereoselectivity in di-*tert*-butylsilylene-directed α-galactosylation. *J. Org. Chem.* **2016**, *81*, 9086−9104.
(36) Hagen, B.; van Dijk, J. H. M.; Zhang, Q.; Overkleeft, H. S.; van der Marel, G. A.; Codee, J. D. C. Synthesis of the *Staphylococcus aureus* strain M capsular polysaccharide repeating unit. *Org. Lett.* **2017**, *19*, 2514−2517.
(37) Dondoni, A.; Marra, A. Recent applications of thiol-ene coupling as a click process for glycoconjugation. *Chem. Soc. Rev.* **2012**, *41*, 573−586.
(38) Although this yield is somewhat lower than the overall yield for the same transformation on the corresponding C-3-*O*-benzoate substrate (see ref 22), the ensuing protecting group manipulations proceeded better with the C-3-acetyl synthon.
(39) Compain-Batissou, M.; Mesrari, L.; Anker, D.; Doutheau, A. Anchimeric assistance by the anomeric phenylthio group in the nucleophilic substitution of a 6-*O*-trifluoromethanesulfonyl-β-D-galactopyranoside. *Carbohydr. Res.* **1999**, *316*, 201−205.
(40) Pozsgay, V. A new strategy in oligosaccharide synthesis using lipophilic protecting groups: synthesis of a tetracosasaccharide. *Tetrahedron: Asymmetry* **2000**, *11*, 151−172.
(41) Use of the corresponding AAT donor with a 3-*O*-benzyloxymethyl ether led to the formation of the desired trisaccharide in poor yield (25%) and stereoselectivity (α:β = 3:1).
(42) The only side product observed in this reaction was the 1,1-linked hexasaccharide.
(43) Lu, L.-D.; Shie, C.-R.; Kulkarni, S. S.; Pan, G.-R.; Lu, X.-A.; Hung, S.-C. Synthesis of 48 disaccharide building blocks for the assembly of a heparin and heparan sulfate oligosaccharide library. *Org. Lett.* **2006**, *8*, 5995−5998.
(44) Ochiai, H.; Huang, W.; Wang, L. Expeditious chemoenzymatic synthesis of homogeneous *N*-glycoproteins carrying defined oligosaccharide ligands. *J. Am. Chem. Soc.* **2008**, *130*, 13790−13803.
(45) Kwon, Y.-U.; Soucy, R. L.; Snyder, D. A.; Seeberger, P. H. Assembly of a series of malarial glycosylphosphatidylinositol anchor oligosaccharides. *Chem. - Eur. J.* **2005**, *11*, 2493−2504.
(46) Tian, W. Q.; Wang, Y. A. Mechanisms of Staudinger reactions within density functional theory. *J. Org. Chem.* **2004**, *69*, 4299−4308.
(47) Lin, F. L.; Hoyt, H. M.; Halbeek, H. V.; Bergman, R. G.; Bertozzi, C. R. Mechanistic investigation of the Staudinger ligation. *J. Am. Chem. Soc.* **2005**, *127*, 2686−2695.
(48) TEMPO-mediated oxidation. In *Oxidation of primary alcohols to carboxylic acids a guide to current common practice*; Tojo, G., Fernandez, M. I., Eds.; Springer-Verlag: New York, 2007; p 116, Vol. *XVI*.
(49) Overberger, C. G.; Anselme, J.-P. A Convenient synthesis of phenyldiazomethane. *J. Org. Chem.* **1963**, *28*, 592−593.
(50) Clausen, M. H.; Madsen, R. Synthesis of hexasaccharide fragments of pectin. *Chem. - Eur. J.* **2003**, *9*, 3821−3832.
(51) Avci, F. Y.; Kasper, D. L. How bacterial carbohydrates influence the adaptive immune system. *Annu. Rev. Immunol.* **2010**, *28*, 107−130.
(52) Avci, F. Y.; Li, X.; Tsuji, M.; Kasper, D. L. Carbohydrates and T cells: A sweet twosome. *Semin. Immunol.* **2013**, *25*, 146−151.
(53) Goldblatt, D.; Plikaytis, B. D.; Akkoyunlu, M.; Antonello, J.; Ashton, L.; Blake, M.; Burton, R.; Care, R.; Durant, N.; Feavers, I.; Fernsten, P.; Fievet, F.; Giardina, P.; Jansen, K.; Katz, L.; Kierstead, L.; Lee, L.; Lin, J.; Maisonneuve, J.; Nahm, M. H.; Raab, J.; RomeroSteiner, S.; Rose, C.; Schmidt, D.; Stapleton, J.; Carlone, G. M. Establishment of a new human pneumococcal standard referenceserum, 007sp. *Clin. Vaccine Immunol.* **2011**, *18*, 1728−1736.
(54) González Aznar, E.; Cabrera Arias, R. A.; Ramírez Bencomo, F.; Fajardo Sánchez, A. R.; Acevedo Groguez, R. Identity of the "Quimi-Vio" Streptococcus pneumoniae vaccine using the Dot Blot technique using monoclonal antibodies against the capsular polysaccharides 1,5, 6B, 14 and 19F of the bacterium. *Bionatura* **2017**, *2*, 248−253.
(55) Mayer, M.; Meyer, B. Group epitope mapping by saturation transfer difference NMR to identify segments of a ligand in direct contact with a protein receptor. *J. Am. Chem. Soc.* **2001**, *123*, 6108−6117.
(56) Similar analyses based on trNOESY experiments were not applied to **2**−**4**, because intense negative NOEs in the free state at 800 and at 600 MHz were observed, which makes it difficult to discriminate between NOEs and trNOEs in the presence of the antibody.
(57) Haji-Ghassemi, O.; Blackler, R. J.; Young, N. M.; Evans, S. V. Antibody recognition of carbohydrate epitopes. *Glycobiology* **2015**, *25*, 920−952.
(58) Evans, S. V.; Sigurskjold, B. W.; Jennings, H. J.; Brisson, J.-R.; To, R.; TseW, C.; Altman, E.; Frosch, M.; Weisgerber, C.; Kratzin, H. D.; Klebert, S.; Vaesen, M.; Bitter-Suermann, D.; Rose, D. R.; Young, N. M.; Bundlev, D. R. Evidence for the extended helical nature of polysaccharide epitopes. The 2.8 A resolution structure and thermodynamics of ligand binding of an antigen binding fragment specific for D-(2−8)-polysialic acid. *Biochemistry* **1995**, *34*, 6737−6744.
(59) Vyas, N. K.; Vyas, M. N.; Chervenak, M. C.; Johnson, M. A.; Pinto, B. M.; Bundle, D. R.; Quiocho, F. A. Molecular recognition of oligosaccharide epitopes by a monoclonal Fab specific for Shigella flexneri Y lipopolysaccharide: X-ray structures and thermodynamics. *Biochemistry* **2002**, *41*, 13575−13586.
(60) Vulliez-Le Normand, B.; Sau, F. A.; Phalipon, A.; Bélot, F.; Guerreiro, C.; Mulard, L. A.; Bentley, G. A. Structures of synthetic O-antigen fragments from serotype 2a Shigella flexneriin complex witha protective monoclonal antibody. *Proc. Natl. Acad. Sci. U. S. A.* **2008**, *105*, 9976−9981.

DOI: 10.1021/acscentsci.9b00454
ACS Cent. Sci. 2019, 5, 1407−1416